Article

Particle-Scale Investigation of PAH Desorption Kinetics and Thermodynamics from Sediment

Upal Ghosh, Jeffrey W. Talley, and Richard G. Luthy

Environ. Sci. Technol., **2001**, 35 (17), 3468-3475• DOI: 10.1021/es0105820 • Publication Date (Web): 28 July 2001

Environ. Sci. Technol. **2001**, *35,* 3468−3475

Particle-Scale Investigation of PAH Desorption Kinetics and Thermodynamics from Sediment

UPAL GHOSH,[†]
JEFFREY W. TALLEY,[‡] AND
RICHARD G. LUTHY*,[†]

Department of Civil and Environmental Engineering, Stanford University, Stanford, California 94305-4020, and Environmental Laboratory, U.S. Army Engineer Research and Development Center, Vicksburg, Mississippi 39180

Dredged sediment from Milwaukee Harbor showed two primary classes of particles in the <2 mm size range: a lighter-density coal- and wood-derived fraction with 62% of total PAHs and a heavier-density sand, silt, and clay fraction containing the remaining 38% of the PAHs. Room-temperature PAH desorption kinetic studies on separated sediment fractions revealed slow desorption rates for the coal-derived particles and fast desorption rates for the clay/silt particles. The effect of temperature on PAH release was measured by thermal program desorption mass spectrometry to investigate the desorption activation energies for PAHs on the different sediment particles. Three activated diffusion-based models and an activated first-order rate model were used to describe the thermal desorption of PAHs for four molecular weight classes. PAH binding with the coal-derived particles was associated with high activation energies, typically in the range of 115−139 kJ/mol. PAHs bound to the clay/silt material had much lower activation energy, i.e., in the range of 37−41 kJ/mol for molecular weight 202. Among the desorption models tested, a spherical diffusion model with PAHs located like a rind on the outer 1−3 μm region best described the PAH thermal desorption response for coal-derived particles. This internal PAH distribution pattern on coal-derived particles is based on prior direct measurement of PAH locations at the subparticle scale. These studies reveal that heterogeneous particle types in sediment exhibit much different amounts and binding of PAHs. PAHs associated with coal-derived particles aged over several decades in the field appear to be far from reaching an equilibrium sorption state due to the extremely slow diffusivities through the polymer-like coal matrix. These results provide an improved mechanistic perspective for the understanding of PAH mobility and bioavailability in sediments.

Introduction

The release of soil- or sediment-bound hydrophobic organic compounds (HOCs), including polycyclic aromatic hydrocarbons (PAHs), from the solid to the aqueous phase typically results in an initial period of rapid release, followed by a period with much slower loss of contaminant from the solid (*1*−*3*). This biphasic pattern makes it difficult to assess contaminant availability and toxicity based on total contaminant concentrations alone. The fraction of such contaminants that are strongly bound and desorb slowly may pose less threat to human health and the environment. But the implementation of this concept is hindered by lack of mechanistic understanding that links slow desorption to reduced bioavailability.

Many prior studies have investigated organic compound desorption kinetics or equilibria from bulk sediments and used such data to infer possible desorption mechanisms. Direct measurement of PAH contaminant location on sediments at the microscale has not been possible until recently (*4*). Hence, past methods that employed bulk techniques for assessing sorption and sequestration of HOCs, like PAHs, on geosorbents do not provide information about where toxic contaminants are located, how they are associated, nor what fundamental mechanisms govern HOC sorption. These deficiencies point to the need for improved understanding of sequestration processes and the effect of such processes on sorption, bioavailability, and toxicity of PAHs in geosorbents (*5*, *6*). Improved mechanistic knowledge of the nature of PAH association with sediment particles can result in much better understanding of PAH availability and can improve decision making for setting sediment quality criteria, defining cleanup goals, selecting appropriate treatment technologies, and helping to set priorities among environmental problems.

A physical mechanism that may explain slow desorption is slow diffusion, which may occur either through an organic matter matrix or through and along the walls of intraparticle pores, possibly with a hydrophobic wall coating. Organic-matter diffusion models with shallow penetration depths on the order of a micron to tens of nanometers have been proposed (*7*−*9*). Many intraparticle diffusion-based models (*10*−*13*) assume a particle-scale pore diffusion process, although direct physical evidence is lacking on typical depths of penetration for contaminants in field sediments. In a previous study (*4*) we reported the first microscale observations of PAH distribution within the interior of sediment particles, which showed that the majority of the PAHs in dredged Milwaukee Harbor sediment were present in the near surface regions (<5 μm) of coal-derived particles. Those observations suggested that slow desorption in the study sediment was related to sorption in coal-derived particles, possibly with shallow diffusional distances compared to the particle scale.

In our earlier work (*4*) we showed that Milwaukee Harbor dredged sediment particles comprised two principal fractions in each size range: (1) a lighter-density coal- and wood-derived fraction (contributing 5% of the sediment weight and 62% of total PAHs) and (2) a heavier-density sand, silt, and clay fraction (contributing 95% of the sediment weight and 38% of total PAHs). Desorption kinetic studies were carried out at room temperature using the separated sediment components to investigate the nature of the PAH sorption process in the two primary sediment particle types. Those studies provided information on the relative contribution of sediment particle types to the fast and slow desorption of PAHs. We report in this paper results of the effect of temperature on desorption rate as measured by thermal program desorption mass spectrometry (TPD-MS). We investigate the thermodynamics of the sorption process for the primary sediment particle types and test four desorption models to describe the process of PAH release from the

* Corresponding author phone: (650)725-9170; fax: (650)723-3164; e-mail: luthy@stanford.edu.
[†] Stanford University.
[‡] Current address: Department of Civil Engineering and Geological Sciences, University of Notre Dame.

10.1021/es0105820 CCC: $20.00
Published on Web 07/28/2001

sediment particles. The experimental data and model fitting allowed the estimation of the desorption activation energy for the different sediment components revealing information about the PAH sorption mechanism for the principal particle types in the sediment that contain PAHs.

Model Development and Parameter Estimation

An activated first-order rate model and three activated diffusion-based models with different diffusional geometries were evaluated to describe the thermal desorption of PAHs from sediment particles.

First-Order Model. A first-order desorption model to describe PAH loss from sediment particles is described in eq 1

$$\frac{dC}{dt} = -kC \tag{1}$$

where C is the concentration of PAH in the particle at any time t (mass PAH/mass particle), and k is the first-order rate constant. During thermal program desorption, the increase in k with temperature can be described by an Arrhenius function shown in eq 2

$$k = k_o e^{-E_a/RT} \tag{2}$$

where k_o is a preexponential factor, E_a is the activation energy (kJ/mol), R is the universal gas constant, and T is temperature in K. The value of k_o can be expressed as a function of a desorption rate constant at 20 °C (k_{20C}) and substituted in eq 1 as shown in eq 3.

$$\frac{dC}{dt} = -Ck_{20C}e^{(E_a/R)(1/293-1/T)} \tag{3}$$

It was shown elsewhere (*14*) that the two parameters k_{20C} and E_a are highly correlated, and unique values of both cannot be estimated simultaneously from a single set of thermal program desorption data. Therefore, an independent measure of the parameters is necessary. This is possible through desorption kinetic tests conducted at a fixed temperature to estimate k_{20C}. With k_{20C} known, the desorption activation energy can be estimated by fitting eq 3 to thermal program desorption data.

Diffusion-Based Models. Geosorbent organic matter is thought to have a macromolecular structure, and slow diffusion through macromolecular organic matter is often considered similar to polymer diffusion (*15*, *16*). Polymer diffusion is understood to proceed through a sequence of two steps: the creation of a hole in the polymeric matrix (an endothermic process) and the accommodation of a solute molecule in that hole (an exothermic process). The overall sorption process is exothermic. The sorption of HOCs to organic polymers is a thermodynamically favored process (*16*, *17*). Sorption of PAHs on coal-derived particles is expected to resemble polymer sorption due to the physical structure of coal, which is described as a porous macromolecular gel (*18*) that swells on interaction with solvents (*19*) and shows a glass transition temperature of about 325 °C (*20*). In addition, there is evidence to suggest penetration of PAH molecules within aromatic structures present in coals. Nuclear magnetic resonance studies on interactions between PAHs and coals reveal that PAHs penetrate within the coal matrix and interact with the coal macromolecules through associative bonding such as $\pi-\pi$ electrodynamic interactions (*21*). Such molecular interactions between a PAH molecule and the aromatic rings within a coal polymer can enhance the sorptive binding of a PAH molecule.

The temperature dependence of polymer diffusion is governed by the activation energy required by the molecules to jump from one hole to another in the polymer matrix. Therefore, the effect of temperature on diffusivity can be expressed by an Arrhenius function as in eq 5 (*15*, *16*, *22*)

$$D = D_0\, e^{-E_a/RT} \tag{4}$$

where D = diffusivity through organic matter (cm^2/s), D_0 = preexponential factor (cm^2/s), E_a = activation energy for diffusion in polymer (kJ/mol), and R = universal gas constant (kJ/mol-K). Similar to eq 3, eq 4 can be expressed in terms of diffusivity calculated at 20 °C (D_{20C}) as shown in eq 5.

$$D = D_{20C}e^{(E_a/R)(1/293-1/T)} \tag{5}$$

It is instructive to note how the change in D with temperature responds to different E_a values for a given value of D at room temperature. For an unactivated process with $E_a = 0$, D/D_{20C} equals 1 and does not change with increasing temperature. However, with increasing value of E_a, D/D_{20C} increases rapidly with temperature. Typical values of E_a for diffusion of small organic molecules through polymeric materials average 60 kJ/mol (*16*, *17*). For such values of E_a, the value of D/D_{20C} increases by nearly 5 orders of magnitude as the temperature is increased from room temperature to 300 °C (see Figure S2 in Supporting Information). Due to the high sensitivity of diffusivity to temperature during thermal desorption, other minor factors that could possibly affect the diffusion process such as non-Fickian effects have been neglected in this modeling. For example, the effect of non-Fickian diffusion of methylene chloride in glassy polystyrene could be accounted for by an increase in the diffusivity by a factor of only two or three (*23*).

Three diffusion geometries were modeled in this study:

1. Diffusion from a Sheet with Uniform Initial PAH Concentration. This model conceptualizes desorption from a thin layer of organic matter coating on inert mineral surfaces with diffusion occurring from the exposed planar surface. Direct evidence of such desorption regime was reported in an earlier study (*4*) wherein infrared microspectroscopic work in combination with microprobe laser desorption-laser ionization mass spectrometry revealed the existence of patchy organic matter coatings with sorbed PAHs on mineral particles in the sediment. Diffusion of PAHs from a planar source can be described by a one-dimensional diffusion equation as shown below.

$$\frac{\partial C}{\partial t} = D(t)\frac{\partial^2 C}{\partial x^2} \tag{6}$$

Here, $D(t)$ is a function of time as temperature increases linearly with time, and a transformation of the variable is required before an analytical solution can be applied. A convenient transformation involves a transformed time variable τ as shown in eq 7 (*24*). Thus, eq 6 reduces to eq 8, for which an analytical solution is available to describe the mass remaining in a plane sheet for long times with one surface exposed to an infinite sink (eq 9) (*24*).

$$d\tau = D(t)dt \rightarrow \tau = \int_0^t D(t')dt' \tag{7}$$

$$\frac{\partial C}{\partial \tau} = \frac{\partial^2 C}{\partial x^2} \tag{8}$$

$$\frac{M_\tau}{M_o} = \frac{8}{\pi^2}\sum_{n=0}^{\infty}\frac{1}{(2n+1)^2}\exp\left\{-\frac{1}{a^2}(2n+1)^2\pi^2\tau\right\} \tag{9}$$

where M_τ = PAH remaining in the plane sheet at transformed time τ, M_o = initial PAH mass in the plane sheet, and τ/a^2

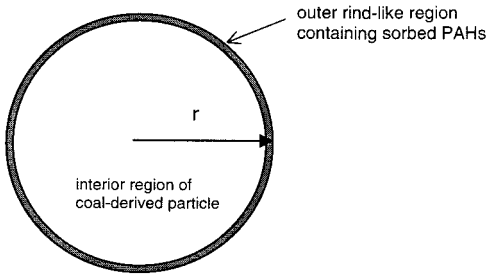

FIGURE 1. Schematic cross-section of model coal-derived particle showing sorbed PAHs within a rind-like region on the outer portion of the particle.

is obtained by dividing eq 7 by a^2 and integrating numerically for the time period of simulation. The diffusive length scale a is constant. During thermal program desorption the value of D/a^2 changes with temperature as in eq 5, and temperature increases at the rate of 10 °C/min. The value of D_{20C}/a^2 is estimated from a room-temperature desorption kinetics study.

2. Fully Penetrated Spherical Particles with Uniform initial PAH Concentration. A commonly used diffusion model for release of organic contaminants from geosorbents assumes a spherical geometry. Using the transformed variable, τ, an analytical solution for spherical geometry for long times is provided by Crank (*24*) for the condition of uniform initial concentration within the sphere, as shown in eq 10

$$\frac{M_\tau}{M_o} = \frac{6}{\pi^2}\sum_{n=1}^{\infty}\frac{1}{n^2}e^{(-n^2\pi^2\tau/a^2)} \qquad (10)$$

where M_τ = mass of PAH remaining in particle at transformed time τ, M_0 = mass of PAH in particle at time 0, τ/a^2 is determined as in the case for the sheet model.

3. Spherical Particles with PAHs Located Like a Rind on the Outer Regions of Sorbent Particles. This model assumes that PAH sorption on the outer regions of a spherical polymeric material, such as coal particles in sediments as shown schematically in Figure 1. In an earlier study (*4*) we showed that PAHs on coal-derived particles in Milwaukee Harbor dredged sediment are located within the near surface (<5 μm) region. Therefore a fully penetrated spherical geometry for organic contaminant diffusion may not be appropriate for describing the desorption of PAHs from such sediment coal-derived particles. Modeling of contaminant diffusion from geosorbents with nonuniform initial concentrations has not been done in the past due to the lack of direct evidence for the penetration depth of contaminants within geosorbent particles and lack of knowledge of the initial concentration profile existing within the geosorbent particle. In the case of PAHs located like a rind on the outer regions of a sorbent particle, convenient analytical solutions are not available, and a rigorous numerical treatment is required. A finite difference solution scheme was adopted to solve the diffusion equation in spherical coordinates with central difference in space and weighted average in time. The rind model was based on diffusive release of PAHs that had penetrated the coal-derived particles. The penetration profile was generated by applying a particle diffusion model to create a PAH penetration depth of 1−3 μm as observed through direct spectroscopic measurement of sectioned particles. The numerical model was coded in Visual Fortran (Digital Equipment Corporation) and run on an IBM-compatible personal computer.

Materials and Methods

The sediment used in this study was obtained from the Milwaukee Harbor Confined Disposal Facility (CDF) operated by the Milwaukee Harbor Port Authority. These sediments originated from Milwaukee Harbor during the process of dredging to maintain waterway navigability. Dredged sediment environmental issues include the potential for release of contaminants from such CDF sites, closure requirements (*25*), and the feasibility of composting biotreatment to reduce PAH concentrations and convert the dredged sediment to material suitable for offsite beneficial uses (*26*). The sediment was composed primarily of silt and clays (61 wt % < 63 μm), sand (34 wt % 63−1000 μm), and carbonaceous matter derived from coal and wood (5 wt %). The total PAH concentration in the sediment was 90 mg/kg, the majority of which (62%) was found in the coal-derived fraction (*4*). Figure S1 (Supporting Information) shows coal- and wood-derived particles from Milwaukee Harbor sediments. Historic coal coking and gasification units located near the Milwaukee Harbor and coal shipping operations in the harbor are thought to be sources of coal in the sediment at this site (*27*). Additional information about the sediment geochemistry has been reported earlier (*4*).

Particle Separation and PAH Analysis. Wet sieving was performed to separate the sediment into four size fractions (>1000 μm, 1000−250 μm, 250−63 μm, and <63 μm). Each size fraction was further separated into lighter and heavier density fractions using entrainment or $CsCl_2$ salt solution as explained elsewhere (*4*). The heavier density fraction comprised sand, silt, and clays. The lighter-density fraction comprised primarily coal- and wood-derived particles. The coal- and wood-derived particles in the lighter density fraction were further separated by density and analyzed for PAHs. Coal-derived particles comprised 82 wt % of this fraction and contained 95% of the PAHs. Thus, the lighter density material is composed predominantly of coal-derived material, and the remaining wood-derived fraction plays an insignificant role as far as PAHs are concerned. In the rest of this paper we call the lighter density fraction the coal-derived fraction due to the predominance of coals. PAH extraction and analysis were carried out using EPA standard methods and are explained in a previous paper (*4*).

PAH Desorption Study. Fixed temperature PAH desorption kinetic studies using Tenax resin beads were conducted using the original sediment and separated fractions. Desorption tests followed procedures used previously (*17*) and are explained in detail elsewhere (*4*).

Thermal Program Desorption Study. A quadrupole mass spectrometer (MS) with a direct insertion probe manufactured by Thermoquest was used for thermal program desorption (TPD) measurements. The TPD-MS instrument was configured so that a sample could be directly inserted into the ion volume of the MS. This allows for efficient transfer of desorbed compounds as well as increased sensitivity. The sample is inserted into the mass spectrometer in a 1 mm diameter glass vial held at the tip of the probe. The temperature of the probe containing the sample glass vial is then increased according to a predetermined temperature ramp. The volatilized compounds are ionized and selectively filtered in the quadrupole and detected in the mass spectrometer. The high sensitivity of the TPD-MS enabled milligram quantities of samples to be analyzed. Triplicate runs were conducted and averaged for each sample. Within each TPD run, the raw ion count is proportional to the molecular flux in the ion volume. Thus, the ion count measured at any time is proportional to the rate of release of PAHs from the sample vial. A detailed description of the TPD instrument and use for PAH measurement on solids is presented elsewhere (*14*).

Results and Discussion

Measurement of Desorption Rates at Room Temperature. Desorption experiments were performed with the whole

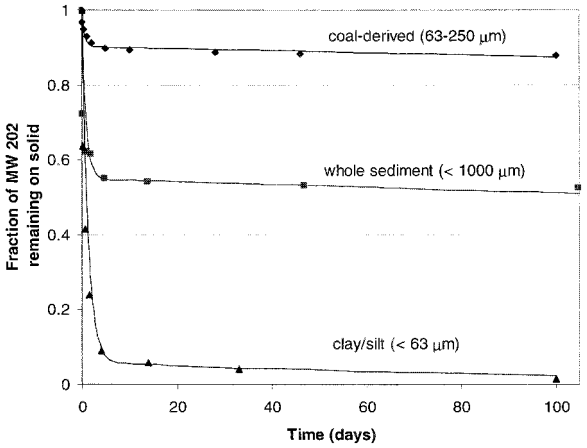

FIGURE 2. Desorption of PAH molecular weight 202 (fluoranthene and pyrene) from Milwaukee Harbor sediment at 20 °C showing faster desorption from heavier-density clay/silt fraction compared to the lighter-density coal-derived fraction. The lines show fitted dual first-order model.

sediment, the coal-derived fraction (63−250 μm), and the clay/silt fraction (<63 μm). The results of these desorption experiments showing release of total EPA priority pollutant PAHs from Milwaukee Harbor dredged sediments have been presented earlier (*4*). In this paper, detailed analysis and modeling results are presented for individual PAH molecular weights: 178 (phenanthrene and anthracene), 202 (fluoranthene and pyrene), 228 (chrysene and benzo[*a*]anthracene), and 252 (benzo[*b*]fluoranthene, benzo[*k*]fluoranthene, and benzo[*a*]pyrene). The aqueous desorption results for MW 202 from the whole sediment, separated coal- and wood-derived particles, and clay/silt particles are shown in Figure 2. This test shows that for the whole sediment approximately 45% of MW 202 were released quickly, and approximately 55% were strongly bound. The PAHs associated with the coal-derived fraction appear to be bound very strongly, as only about 10% of the PAHs in this fraction was released in 100 days. In contrast, desorption data from the heavier clay/silt fraction indicate a higher availability with nearly 90% of the initial PAHs in this fraction readily desorbing in 4 days and more than 98% in 100 days. Thus, PAHs on coal-derived particles comprise the strongly bound fraction of the whole sediment. The desorption rates of the other PAHs exhibited a pattern similar to that for MW 202.

Estimation of Desorption Rate Constants. A phenomenological two compartment model comprising both fast and slow desorbing PAH compartments in sediment describes the desorption kinetics observed in Figure 2

$$\frac{C}{C_o} = fe^{-k_f t} + (1-f)e^{-k_s t} \tag{11}$$

where C = PAH concentration in sediment, C_o = initial PAH concentration in sediment, f = fraction of fast desorbing pool in sediment, k_f = first-order rate constant for fast component, and k_s = first-order rate constant for slow component.

Similar two compartment models have been used previously to model the desorption of hydrophobic organic compounds from sediments (*17*, *28*). The model was fitted to the normalized PAH desorption data to estimate the room-temperature desorption rate constants. A nonlinear curve fitting routine based on the Marquardt−Levenberg algorithm was used to fit the nonlinear model to the measured data on PAH desorption. Three parameters were estimated for each set of desorption data: the first-order desorption coefficients for fast and slow pools (k_f and k_s) and the fast pool PAH fraction (f). The fraction of PAHs in the slow desorbing pool was calculated as $(1 - f)$. The estimated parameters for PAH molecular weight 202 desorption from the clay/silt fraction (<63 μm) and the coal-derived (63−250 μm) sediment fraction are presented in Table 1.

Early work on chromatography (*29*) suggested that first-order mass transfer could be used to approximate diffusion. An approximate correlation between a first-order rate constant and the diffusion coefficient is (*30*, *31*)

$$k = 15(D_e/a^2) \tag{12}$$

where k = first-order rate constant, D_e = effective diffusivity, and a = diffusional distance.

Values of D/a^2 calculated from k_f and k_s are shown in Table 1. The desorption kinetics experiments were conducted at room temperature (20 °C), and these values of D/a^2 can be used for D_{20C} in eq 5 to model the change in diffusivity with rise in temperature. As shown in Table 1, there is a nearly 2−3 orders of magnitude difference in desorption rates for the slow and fast fraction for each particle type. The fast rate constants for coal derived particles were in the same order of magnitude as the fast rate constants for clay/silt particles. It is not clear however if this implies similar desorption mechanisms. For the coal-derived particles, the major desorbing fraction is the slow fraction, and for the clay/silt particles the fast desorbing fraction is the dominating fraction.

Thermal Program Desorption Results and Interpretation. Thermal program desorption experiments were conducted using coal-derived (63−250 μm) and clay/silt (<63 μm) sediment fractions to investigate the release of PAHs as a function of temperature. In each experiment an approximately 1−2 mg sample was placed in a TPD glass vial and inserted into the TPD-MS. The sample amount was small enough so that no retardation due to interparticle sorption was observed. A temperature ramp of 10 °C/min was used from a starting temperature of 30 °C, and the test was run to a maximum temperature of 400 °C. The temperature ramp was initiated immediately after sample introduction. The MS signal was collected in a selective ion-monitoring (SIM) mode with a sampling frequency of approximately 80/min resulting in nearly 3000 data points for each run. The data were smoothed by averaging every five consecutive values, which reduced data noise. Figure 3a shows a smoothed TPD response obtained by such data processing for PAH mass numbers 178, 202, 228, 252, 276, and 278 for clay/silt particles (<63 μm) from Milwaukee Harbor sediment. Ion counts plotted on the *y*-axis are proportional to the instantaneous rate of release of PAHs from the sample. The area under each curve represents the total mass of the compound released over the time period of desorption when the *x*-axis is expressed in time units. Thus, dividing the instantaneous rate by the area under the TPD curve and averaging the three

TABLE 1. Parameters f, k_f, and k_s Estimated from PAH Molecular Weight 202 Desorption Data of Coal-Derived Fraction and Clay/Silt Fraction of Sediment Shown in Figure 2

particle type	f (fast fraction)	k_f (s^{-1})	k_s (s^{-1})	$[D/a^2]_f$ (s^{-1})	$[D/a^2]_s$ (s^{-1})
coal-derived (63−250 μm)	0.09	2.1×10^{-5}	3.6×10^{-9}	1.4×10^{-6}	2.4×10^{-10}
clay/silt (<63 μm)	0.94	9.25×10^{-6}	5.8×10^{-8}	6.2×10^{-7}	3.9×10^{-9}

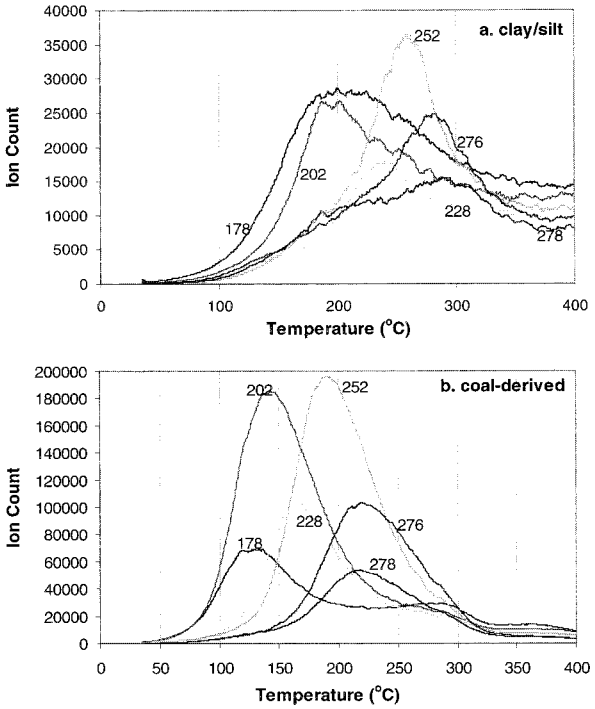

FIGURE 3. TPD response of PAH mass numbers 178 (phenanthrene and anthracene), 202 (fluoranthene and pyrene), 228 (chrysene and benzo[*a*]anthracene), 252 (benzo[*b*]fluoranthene, benzo[*k*]fluoranthene, and benzo[*a*]pyrene), 276 (benzo(g,h,i)perylene and indeno-(1,2,3-c,d)pyrene), and 278 (dibenzo(a,h)anthracene) for (a) clay/silt particles (<63 μm) and (b) coal-derived particles (63−250 μm) from Milwaukee Harbor sediment.

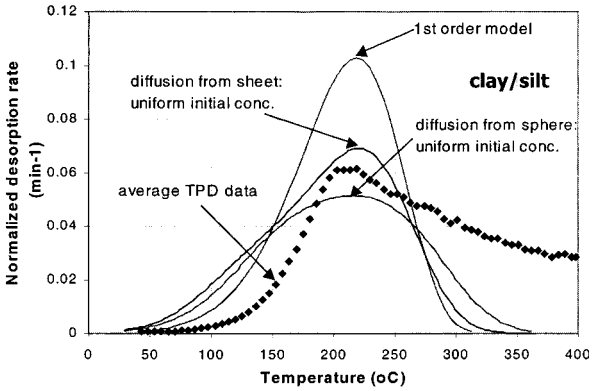

FIGURE 4. Average TPD-MS signal for PAH molecular weight 202 (fluoranthene and pyrene) and prediction based on activated first-order and two activated diffusion models for release from clay/silt particles.

replicates, we obtain the normalized rate or fractional release rate curve as shown in Figures 4 and 5.

The TPD response of the same PAHs for sediment coal-derived fraction (63−250 μm) is shown in Figure 3b. In Figure 3b there is no major discontinuity in the desorption profile which could have been indicative of a glass transition point for the polymeric coal. If evident at all, there could be a minor indication of a sudden change in slope near the tailing end of the TPD curves near 300 °C for all PAHs in Figure 3b. Reported values of glass transition temperatures for coals are above 300 °C (*20*, *32*). For both types of particles in Figure 3, the TPD response does not reach a zero value in the tailing edge of the peak. The relative effect is more pronounced for the clay/silt particles for which the overall TPD response is small. Two possible causes for this behavior are as follows: increasing TPD-MS baseline with increasing temperature and

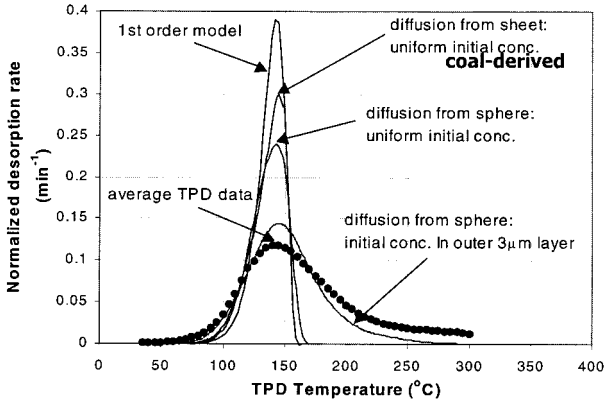

FIGURE 5. Average TPD-MS signal for PAH molecular weight 202 (fluoranthene and pyrene) and prediction based on activated first-order model and three activated diffusion models for release from coal-derived particles. Among the four models tested, the model incorporating nonuniform initial concentration within the coal-derived particle best simulates the spread of the TPD curve.

beginning of pyrolysis of organic matter at temperatures above 350 °C.

There are two major differences in the TPD responses from coal-derived and clay/silt particles as shown in Figure 3a,b. First, the TPD signal response for coal-derived particles is nearly 1 order of magnitude larger compared to that of the clay/silt particles. This difference is due to the much higher concentration of PAHs present in the coal-derived particles in the sediment as measured by extraction and analysis (*4*). Second, the peak temperatures of TPD response for clay/silt particles are approximately 70 °C higher than for the corresponding peaks for coal-derived particles. The higher temperatures required to release the PAHs from the clay/silt particles compared to coal-derived particles may appear counterintuitive based on our knowledge of faster desorption rates from clay/silt. However, a closer examination of the possible release mechanism reveals that diffusivity increases much more slowly with temperature for low activation energies.

The nature of the desorption process for PAHs from the different sediment particle types was investigated by applying the four desorption models to fit the TPD-MS data. The fourth model, which is more appropriate to describe polymer diffusion through coal-type particles, was not applied to the clay/silt material. All four models used an Arrhenius relationship to describe the effect of temperature on desorption rate or diffusivity as shown in eqs 2 and 5.

Application of the Rind Model. The rind model was first run in the penetration mode to form the initial concentration profile based on reasonable assumptions about the contamination history. While the exact history of contamination of the coal-derived particles in the sediment is not known, we know that (1) the PAHs are not inherently present in the source coal based on the measurement of very low levels of extractable PAHs from virgin coals, e.g., 3 mg/kg for Illinois No. 6 coal, (2) the PAH distribution found in the sediment coals indicate pyrogenic sources for the PAHs, (3) PAH abundance within the particle interior reduces 30-fold at a distance 3−5 μm inside the outer surface (*4*), and (4) the history of coal use and coal processing operations and PAH release in the Milwaukee Harbor region dates back to the early part of the 20th century (*27*, *33*). Based on these observations, the particle sorption profile was simulated by assuming sorption of PAHs onto clean coal particles occurring over a number of years. Two initial concentration profile depths were used: (1) 90% of the contaminants within the outer 1 μm region and (2) 90% of the contaminants within the outer 3 μm region. The depth of penetration is not a

TABLE 2. Fitted Values of Desorption Activation Energies for PAH MW 202 from Clay/Silt and Coal-Derived Particles in Milwaukee Harbor Sediment

	clay/silt (kJ/mol)	coal-derived (kJ/mol)
first order	41	137
sheet diffusion	40	138
spherical diffusion: uniform	37	138
spherical diffusion: nonuniform (1 μm penetration)		133

fitted parameter but based on results from our direct spectroscopic measurement. Results of model fitting using a range of penetration depths are discussed in the Supporting Information. For generating the normalized penetration profile, a linear partitioning between the coal particle surface and water was assumed with arbitrary values for the partition coefficient and aqueous concentration. The reported desorption values are in the units of fractional release rates and therefore are independent of initial mass accumulated in the solid phase. Room-temperature diffusivity was determined by running the desorption model for a constant-temperature condition to simulate the room-temperature desorption data. The room-temperature desorption profile for PAH molecular weights 178, 202, 228, and 252 for coal-derived particles showed a major fraction (75−95%) of each PAH desorbing at a slow rate. Thus, the value of room-temperature diffusivity was estimated by fitting the model desorption profile with the slow-release rate portion of the room-temperature desorption data for coals. The duration of penetration necessary to create the required sorbed profile and also match the room-temperature desorption data was nearly 50 years. This time scale of sorption is comparable to the known contamination history of the harbor sediments. The penetration step was followed by a model run that simulated the temperature program desorption mode where the temperature of desorption increased at 10 °C/min as in the thermal program desorption experiments. The following initial and boundary conditions were used for the numerical solution:

Penetration Phase: Initial condition: $C = 0$ for all r at $t = 0$; and $C = C_0$ at $r = R$ for $t > 0$

Boundary condition: $dC/dt = 0$ at $r = 0$

Desorption Phase: Initial condition: C profile created during penetration phase

Boundary condition: $C = 0$ at $r = R$ for $t > 0$; $dC/dt = 0$ at $r = 0$ for all t

TPD Model Fitting for Clay/Silt Particles. The first three desorption models were used to describe the TPD results of clay/silt particles. The room-temperature desorption rate or diffusive rate was estimated from the aqueous desorption study (Table 1). The predominant rate fraction (fast fraction for clay/silt, and slow fraction for coal-derived) that described the desorption rate of majority of PAHs in the solid phase was used for the desorption model. The activation energy parameter was fitted by trial and error to obtain a desorption peak temperature matching the measured TPD peak. The result of model fitting to TPD response from clay/silt particles is shown in Figure 4 for MW 202 which was the most abundant PAH group present. For ease in comparison, TPD data and model simulations are presented as fractional desorption rates i.e., normalized rates, obtained by dividing desorption rates by total initial PAH mass. All three models provide a reasonable simulation of the peak temperature with estimated activation energy values ranging from 37 to 41 kJ/mol (Table 2). Such low values of desorption activation energy are expected for sorption of PAHs on mineral surfaces and humic matter coated surfaces. However, the shapes of the simulated TPD response differ and do not match well with the data. One reason for the difference is the distorted nature of the TPD data for clay/silt particles, which may be due in part to the relatively low signal, and possible start of pyrolysis of natural organic matter on clays at temperatures above 300 °C.

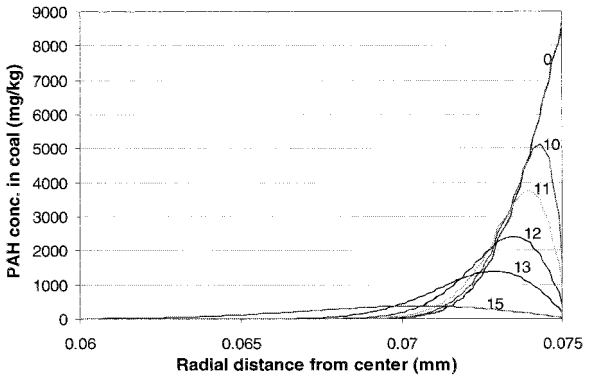

FIGURE 6. Simulated PAH molecular weight 202 concentration profile within a 150 micron diameter coal-derived particle during a thermal program desorption experiment at 10 °C/min showing inward diffusion of PAHs. Numbers indicate minutes during TPD simulation.

TPD Model Fitting for Coal-Derived Particles. The results of fitting the four desorption models to the TPD-MS data for PAH molecular weight 202 on coal-derived particles are shown in Figure 5. All four desorption kinetics models provided high activation energy values ranging between 133 and 138 kJ/mol (Table 2). Such high activation energies are expected for PAH sorption on polymeric organic matter such as coal. Carroll et al. (11) reported an activation energy of 170 kJ/mol for the desorption of PCBs from condensed soil organic matter. Thus, based on all four model fits to fixed temperature desorption data and TPD-MS data, desorption of PAH MW 202 from clay/silt particles is associated with low activation energies (37−41 kJ/mol) compared to coal-derived particles, which are associated with high activation energies (133−138 kJ/mol).

All four desorption models appeared to fit the observed peak temperature of the TPD profile for coal-derived particles reasonably well, giving similar values of activation energies. However, there were major differences in the TPD profiles. The first three models simulated a very narrow peak with a sharp tailing edge of the TPD response. This is caused by the exponential increase in fractional release rates at temperatures above the peak. In contrast, the measured TPD data showed a much wider peak with a slowly reducing tail. Only the spherical diffusion model with a nonuniform initial PAH concentration appeared to simulate the shape of TPD-MS profile well. The modeling revealed that during the TPD process, PAHs which had accumulated on the outer regions of the spherical particle also diffuse increasingly toward the particle interior because of the existing driving force toward the interior and increased diffusivity at higher temperatures. This phenomenon is illustrated in Figure 6 which shows the predicted internal PAH concentration profile during a TPD experiment. As the temperature is increased, PAHs in the outer layers of the spherical particle are desorbed out. However, PAHs in the inner layers continue to diffuse inward due to the negative concentration gradient toward the center of the particle as well. This results in a slowing of the eventual release of PAHs out of the particle and produces the distinctively broader TPD peak and slow release tail of the TPD simulation. Thus, among the four models tested, it appears that the desorption of PAHs from sediment coal-

TABLE 3. Fitted Rates and Activation Energies of Desorption of Four PAH Molecular Weights from Coal-Derived Particles in Milwaukee Harbor Sediments

MW	k (s^{-1})	Dla^2 (s^{-1})	E_a (kJ/mol) first order	E_a (kJ/mol) sheet	E_a (kJ/mol) sphere	penetration = 3 μm		penetration = 1 μm	
						D (cm^2/s)	E_a (kJ/mol)	D (cm^2/s)	E_a (kJ/mol)
178	13.8×10^{-9}	9.3×10^{-10}	135	138	137	5.8×10^{-17}	126	1.3×10^{-17}	120
202	3.6×10^{-9}	2.4×10^{-10}	137	138	138	3.5×10^{-18}	139	0.8×10^{-18}	133
228	2.9×10^{-9}	1.9×10^{-10}	120	122	120	2.3×10^{-18}	124	0.58×10^{-18}	118
252	1.2×10^{-9}	0.7×10^{-10}	115	116	115	0.5×10^{-18}	123	0.17×10^{-18}	116

derived particles is described best by a diffusion model wherein the initial concentration of PAHs is localized within the outer few micron depths of the particle.

To test the effect of PAH molecular weight on the desorption rate and activation energy, the desorption of four PAH molecular weights 178, 202, 228, and 252 from coal-derived particles were studied. The results of model fitting for these four molecular weights using the four desorption models are shown in Table 3. The rind model provided the best data simulation for the four molecular weight groups tested. The estimated activation energies for the four PAH molecular weights on coal-derived particles using the four models range between 115 and 139 kJ/mol without a significant trend based on the choice of model used to fit the data. These values are compared against some recently reported activation energy values in the literature for field materials as shown in Table S3 (Supporting Information). Except for the work by Carroll et al. (*9*) the majority of the reported values for soils and sediments are less than 100 kJ/mol. It has been suggested for organic contaminants that activation energies greater than 60 kJ/mol may correspond to diffusion through a polymeric material (*17*, *34*). The diffusion of toluene in low-density polyethylene, for example, was reported to have an activation energy of 87 kJ/mol (*35*). However, Werth et al. (*36*) have reported high activation energies for diffusion of organic molecules through glassy polymers and amorphous polymers as well as microporous solids. Based on our knowledge of the polymeric nature of coal, and the high activation energy for diffusion, it is most likely that a glassy-polymer like diffusion process governs the sorption of PAHs in the Milwaukee Harbor sediment coal-derived particles.

Implications. Some of the implications of very high activation energies associated with PAH sorption on coals include the following: (1) extremely slow desorption rates and low availability at ambient temperatures and (2) significantly higher rates of release of PAHs with increasing temperature. For example, much slower rates of release of PAHs may be expected in colder climates, compared to warmer ones, and in the guts of cold-blooded animals compared to warm-blooded ones. For an activation energy of 120 kJ/mol, the desorption rate increases by nearly 2 orders of magnitude as the temperature increases from 10 °C to 37 °C.

The extremely small PAH diffusivities in coal-derived particles at ambient temperatures estimated in our work (10^{-17}–10^{-19} cm^2/s) compare well with other reports for which an attempt was made to estimate a diffusivity based on some assumption of a diffusive length scale through an organic polymer. For example, Carroll et al. (*9*) calculated for PCBs D_{eff} values in the range of 10^{-20}–10^{-21} cm^2/s corresponding to diffusion length scales of ~30 nm through polymeric soil organic matter. Pignatello and Xing (*37*) suggested effective diffusivities less than 10^{-17} cm^2/s for EDB, atrazine, and metolachlor desorption from soil organic matter assuming an upper limit of diffusion length scale on the order of the size of clay particles (10^3–10^2 nm). A reported value of

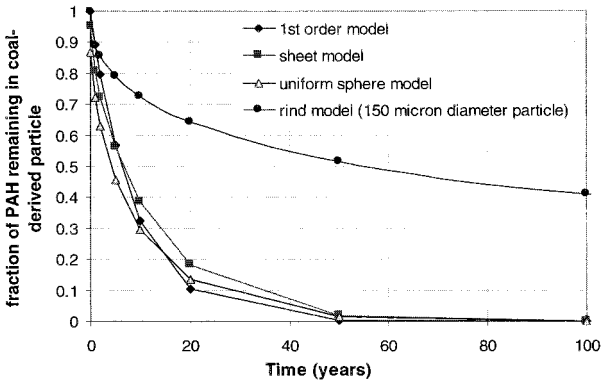

FIGURE 7. Simulated profiles based on four models of fraction of PAH molecular weight 202 remaining in a coal-derived particle during long-term desorption into an infinite sink. Penetration depth used for the rind model was 3 μm.

diffusivity of CCl_4 in poly(vinyl chloride) (a glassy polymer at 25–30 °C) is 10^{-17} cm^2/s (*38*).

Although the fixed temperature desorption rate and peak temperatures during TPD are fitted reasonably well by the four models for coal, adequate discrimination of the correct model and desorption mechanism is necessary for reliable long-term prediction of contaminant release in the field. To illustrate this point, simulations were performed using the four models and the fitted parameters to investigate the long-term release of PAH molecular weight 202 from coal-derived particles into an infinite sink at 20 °C. The fraction of PAH remaining in coal-derived particles over time in years is plotted in Figure 7. The first-order model and two diffusion based models with uniform initial concentration predicted similar desorption profiles showing 80–90% release over 20 years. However, the rind model with an initial PAH concentration on the outer regions predicted a much slower long-term release with 40% remaining even after 100 years. Thus, the nonequilibrium PAH distribution existing within the coal-derived particles results in a much slower long-term release and reduced availability of the contaminants in the field.

We have demonstrated for Milwaukee Harbor sediment that PAHs associated with clay/silt particles desorb faster at room temperature and are characterized by low desorption activation energies, whereas PAHs associated with coal-derived material desorb at a much slower rate at room temperature and are characterized by high desorption activation energies. Coal-derived particles in the sediment, which contain the majority of the PAHs, are in a state of nonequilibrium even after decades of aging in the field due to the extremely slow diffusivities through the polymeric coal-derived material. Long-term desorption from the coal-derived particles is slowed by the internal nonequilibrium condition. The high activation energy required for desorption makes PAHs on coal-derived material strongly bound and relatively unavailable at ambient temperatures. Results of biological treatment and uptake studies supporting this hypothesis are presented elsewhere (*39*). PAHs associated with media having

large activation energies may thus comprise the unavailable PAH fraction in sediments, and these PAHs may pose less risk than PAHs in clay and silt fractions.

Acknowledgments

Funding and technical support for this research was obtained from the Department of Defense through the Strategic Environmental Research and Development Program and the U.S. Army Engineer Research Development Center (ERDC). We thank Samuel Tucker and John S. Furey for their assistance with the thermal program desorption measurements.

Supporting Information Available

Comparison of activation energy values reported in the literature, photograph of coal-derived particles, effect of E_a on change in diffusivity with temperature, aqueous desorption data and model fit for four PAH molecular weight groups for coal-derived particles, and effect of PAH penetration depth on model fitting of TPD data. This material is available free of charge via the Internet at http://pubs.acs.org.

Literature Cited

(1) Guerin, W. F.; Boyd, S. A. *Appl. Environ. Microbiol.* **1997**, *58*, 1504−1512.
(2) Alexander, M. *Environ. Sci. Technol.* **1995**, *29*, 2713−2717.
(3) Loehr, R. C.; Webster, M. T. *J. Hazard. Mater.* **1996**, *50*, 105−128.
(4) Ghosh, U.; Luthy, R. G.; Gillette, J. S.; Zare, R. N. *Environ. Sci. Technol.* **2000**, *34*, 1729−1736.
(5) Luthy, R. G.; Aiken, G. R.; Brusseau, M. L.; Cunningham, S. D.; Gschwend, P. M.; Pignatello, J. J.; Reinhard, M.; Traina, S.; W. J. W., Jr.; Westall, J. C. *Environ. Sci. Technol.* **1997**, *31*, 3341−3347.
(6) NRC *Contaminated Sediments in Ports and Waterways, Cleanup Strategies and Technologies*; National Research Council: Washington, DC, 1997a.
(7) Brusseau, M. L.; Rao, P. S. C. *Crit. Rev. Environ. Control* **1989**, *19*, 33−99.
(8) Pignatello, J. J.; Ferrandino, F. J.; Huang, L. Q. *Environ. Sci. Technol.* **1993**, *27*, 1263−1271.
(9) Carroll, K. M.; Harkness, M. R.; Bracco, A. A.; Balcarel, R. R. *Environ. Sci. Technol.* **1994**, *28*, 253−258.
(10) Ball, W. P.; Roberts, P. V. *Environ. Sci. Technol.* **1991**, *25*, 1237−1249.
(11) Pedit, J. A.; Miller, C. T. *Environ. Sci. Technol.* **1995**, *29*, 1766−1772.
(12) Wu, S.; Gschwend, P. M. *Water Resour. Res.* **1988**, *24*, 1373−1383.
(13) Gong, Y.; Depinto, J. V. *Water Res.* **1998**, *32*, 2518−2532.
(14) Talley, J. W. Ph.D. Dissertation, Carnegie Mellon University, Pittsburgh, 2000.
(15) Cussler, E. L. *Diffusion Mass Transfer in Fluid Systems*; Cambridge University Press: New York, 1995.
(16) TenHulscher, T. E. M.; Cornelissen, G. *Chemosphere* **1996**, *32*, 609−626.
(17) Cornelissen, G.; Noort, P. C. M. v.; Parsons, J. R.; Govers, H. A. *J. Environ. Sci. Technol.* **1997**, *31*, 454−460.
(18) Gorbaty, M. L. *Fuel* **1994**, *73*, 1819−1828.
(19) Larsen, J. W.; Mohammadi, M. *Energy Fuels* **1990**, *4*, 107−110.
(20) Nishioka, M.; Larsen, J. W. *Energy Fuels* **1990**, *4*, 100−106.
(21) Sakurovs, R. *Energy Fuels* **1998**, *12*, 631−636.
(22) Pilorz, K.; Bjorklund, E.; Bowadt, S.; Mathiasson, L.; Hawthorne, S. *Environ. Sci. Technol.* **1999**, *33*, 2204−2212.
(23) Crank, J.; Park, G. S. *Diffusion in Polymers*; Academic Press: London and New York, 1968.
(24) Crank, J. *The Mathematics of Diffusion*; Oxford Science Publisher: Oxford, 1975.
(25) Bowman, D. W.; Brannon, J. M.; Batterman, S. A. U.S. Army Corps of Engineers: Seattle, WA, Feb 26−Mar 1, 1996; pp 378−387.
(26) Bowman, D. W. U.S. Army Corps of Engineers: Detroit District, Detroit, 1999.
(27) Karls, J. F.; Christensen, E. R. *Environ. Sci. Technol.* **1998**, *32*, 225−231.
(28) Ghosh, U.; Weber, A. S.; Jensen, J. N.; Smith, J. R. *J. Soil Contamination* **1999**, *8*, 593−613.
(29) Glueckauf, E.; Coates, J. I. *J. Chem. Soc.* **1947**, *II*, 1315−1321.
(30) Young, D. F.; Ball, W. P. *Water Resour. Res.* **1995**, *31*, 2181−2192.
(31) Brusseau, M. L.; Jessup, R. E.; Rao, P. S. C. *Environ. Sci. Technol.* **1991**, *25*, 134−142.
(32) Leboeuf, E. J.; Weber, W. J. J. *Environ. Sci. Technol.* **1997**, *31*, 1697−1702.
(33) Simcik, M. F.; Eisenreich, S. J.; Golden, K. A.; Liu, S.; Lipiatou, E.; Swackahamer, D. L.; Long, D. T. *Environ. Sci. Technol.* **1996**, *30*, 3039−3046.
(34) Pignatello, J. J. *Reactions and Movement of Organic Chemicals in Soils*; Soil Science Society of America: Madison, WI, 1989.
(35) Saleem, M.; Asfour, A. F. A.; Kee, D. D.; Harrison, B. *J. Appl. Polym. Sci.* **1989**, *37*, 617−625.
(36) Werth, C. J.; McMillan, S. A.; Castilla, H. J. *Environ. Sci. Technol.* **2000**, *34*, 2959−2965.
(37) Pignatello, J. J.; Xing, B. *Environ. Sci. Technol.* **1996**, *30*, 1−11.
(38) Berens, A. R. *Makromol. Chem. Macromol. Symp. (cited in Pignatello & Xing, 1996)* **1989**, *29*, 95−108.
(39) Luthy, R. G.; Ghosh, U.; Gillette, J. S.; Zare, R. N.; Talley, J. W.; Tucker, S. Chemical Speciation and Reactivity In Water Chemistry and Water Technology. *A Symposium in Honor of James J. Morgan*; American Chemical Society: Washington, DC, 2000; pp 497−500.

Received for review January 29, 2001. Revised manuscript received May 25, 2001. Accepted June 8, 2001.

ES0105820